Journal of Economic Theory and Econometrics, Vol. 36, No. 3, Sep. 2025, 1–34

An Empirical Study of Diffusion Models for Non-Ferrous Metal Price Dynamics*

Dokyun An† Seungmoon Choi‡

Abstract This paper empirically investigates the dynamic behavior of non-ferrous metal prices, specifically for copper, aluminum, nickel, and zinc, using a range of continuous-time diffusion models. The study employs maximum likelihood estimation with approximate transition probability density functions to analyze daily price data. Our findings reveal that while price volatility is the dominant factor explaining the dynamics of all four metals, the best-fitting model varies by metal. The GD-GV model, with its generalized volatility function, is found to be the most appropriate for aluminum, whereas the more parsimonious CKLS model provides the best fit for copper, nickel, and zinc. This analysis demonstrates that price dynamics within the non-ferrous metal group are not homogeneous, underscoring the necessity of a flexible, metal-specific modeling approach for accurate price characterization.

Keywords Non-ferrous metal price, diffusion process, maximum likelihood estimation.

JEL Classification C13, C22, Q02.

*We are deeply grateful to the two anonymous reviewers for their thoughtful comments and suggestions. This work was supported by the Basic Study and Interdisciplinary R&D Foundation Fund of the University of Seoul (2021).

†School of Economics, University of Seoul, 163 Seoulsiripdae-ro, Dongdaemun District, Seoul, Republic of Korea 02504. E-mail: dokyunan@gmail.com.

‡School of Economics, University of Seoul, 163 Seoulsiripdae-ro, Dongdaemun District, Seoul, Republic of Korea 02504. E-mail: schoi22@uos.ac.kr.

Received August 22, 2025, Revised September 10, 2025, Accepted September 11, 2025

1. INTRODUCTION

Continuous-time diffusion models, with their flexible drift and volatility functions, have proven to be a powerful tool for capturing the complex dynamics of various financial and economic variables. While early applications in finance can be traced back to the work of Louis Bachelier in his 1900 thesis, these models were more widely utilized following the seminal works of (Black and Scholes, 1973). Over time, their application has expanded to a broader range of commodities, including metals and agricultural products, to analyze price movements and to value related derivatives such as futures and options (e.g., Schwartz, 1997; Dixit and Pindyck, 1994).

A number of preceding studies have attempted to model the behavior of commodity prices. For example, Brennan and Schwartz (1985) and Paddock *et al.* (1988) assumed that commodity prices follow a geometric Brownian motion to value natural resource investment projects. While this simple approach provides a foundation, it is limited in its ability to capture complex price dynamics such as mean-reversion and heteroskedasticity. Other studies have employed alternative econometric models to analyze commodity price movements (Nowman and Wang, 2001). However, many of these approaches often rely on discretized versions of continuous-time models, which can introduce estimation bias (Lo, 1988). A key assumption in many applications is that the chosen diffusion model accurately reflects the true dynamics of the underlying asset. However, as demonstrated by Choi and Lee (2020b) in their study on exchange rates, relying on a single, restrictive model can lead to inaccurate conclusions, as different assets may follow different processes. This highlights the critical need to empirically test various flexible diffusion models to identify which one best describes the price movements of a particular asset.

This study contributes to the literature by applying a range of continuous-time diffusion models to the price dynamics of four major non-ferrous metals: copper, aluminum, nickel, and zinc. These metals were selected from the non-ferrous metal group because they are among the most actively traded and are utilized extensively across various industries. As a result, their prices are closely linked to the global economy. Consequently, understanding the dynamic movements of these metal prices is of great importance. Accurate analysis of their price behavior is essential for relevant businesses to hedge against raw material price risk, for investors to formulate portfolio diversification strategies, and for policymakers to

make informed decisions.

To conduct our analysis, we utilize five univariate time-homogeneous diffusion models: the Vasicek (Vasicek, 1977), CIR (Cox *et al.*, 1985), CKLS (Chan *et al.*, 1992), General Drift and Constant Elasticity of Variance (GD-CEV), and the most general General Drift and General Volatility (GD-GV) model (Choi, 2009). A key methodological contribution is the use of maximum likelihood estimation (MLE) based on the approximate transition probability density function (TPDF), a method developed by (Aït-Sahalia, 2008). This approach overcomes the limitations of discrete-time approximations, which are known to produce biased estimators (Lo, 1988), ensuring the efficiency of our results.

Our empirical findings reveal distinct characteristics among the four metals. While all four prices exhibit heteroskedasticity and volatility clustering, the most appropriate model varies. The analysis suggests that the simple CKLS model is sufficient for describing the dynamics of copper, nickel, and zinc, with little evidence of mean reversion in their drift functions. In contrast, the more complex GD-GV model is required to fully capture the unique dynamics of aluminum, where the additional parameters in its generalized volatility function are statistically significant. This comparative analysis demonstrates that even within the same commodity group, a one-size-fits-all approach is insufficient, and a flexible modeling framework is essential for accurately understanding and characterizing price behavior.

The remainder of this paper is structured as follows. Section 2 presents the data and provides motivation for this study. Section 3 discusses the diffusion models used and the estimation methodology. Section 4 reports the estimation results for each metal and provides a comparative analysis and discussion of the results. Finally, Section 5 offers a brief conclusion.

2. NON-FERROUS METAL PRICE DATA

This study analyzes the daily price movements of four major non-ferrous metals: copper, aluminum, nickel, and zinc. The daily price data for these metals were obtained from Datastream, which provides various price series for the same metal, often with different price levels. To ensure the use of globally recognized and representative prices, we specifically utilized the prices from the London Metal Exchange (LME). The LME is the world's leading center for non-ferrous metal trading. A significant

Data	Copper	Aluminium	Nickel	Zinc
Period	1987.11.20– 2021.7.13	1993.7.14– 2021.7.13	1993.7.20– 2021.7.13	1988.12.01– 2021.7.13
Observations	8,778	7,305	7,301	8,509
Mean	4,337	1,816	13,389	1,692
Minimum	1,318	1,023	3,731	722.8
Maximum	10,449	3,271	54,050	4,603
Std. Dev.	2,454	418.4	7,734	762.7
Kurtosis	1.782	3.235	7.477	3.210
Skewness	0.461	0.821	1.743	0.892

Table 1: Summary Statistics of Non-Ferrous Metal Prices. This table provides descriptive statistics for the daily LME prices of four non-ferrous metals, copper, aluminum, nickel, and zinc, expressed in dollars per ton. The statistics include the data period, number of observations, mean, minimum, maximum, standard deviation, kurtosis, and skewness for each metal. Kurtosis measures the tailedness of the distribution, while skewness measures the asymmetry of the distribution.

portion of global non-ferrous metal transactions is conducted through it, with its quoted prices widely accepted as international benchmarks.

Table 1 presents the descriptive statistics for the daily prices (per ton) of copper, aluminum, nickel, and zinc used in this study. The table provides key statistical measures, including the data period[1], number of observations, mean, minimum, maximum, standard deviation, kurtosis, and skewness for each metal. The kurtosis and skewness coefficients, in particular, indicate departures from a normal distribution, suggesting that these price series exhibit features such as fat tails and asymmetry, which diffusion models are designed to capture. Visual inspection of the time series plots (to be presented later) will further illustrate these characteristics, providing motivation for the application of continuous-time diffusion models.

The average price is notably highest for nickel at $13,389 per metric ton, followed by copper, aluminum, and zinc. Nickel's significantly higher price can be attributed to its complex refining process and its increasing demand in new applications, such as electric vehicle batteries, which has attracted substantial speculative capital. All four metals show a wide gap between their minimum and maximum prices, a trend largely driven by

[1]The reason why the data period differs for each metal is that the starting date for which daily price data was made available is different for each metal.

the sharp increase in commodity prices around 2005, which was fueled by a surge in demand from China's rapid industrialization.

For each metal, three types of graphs have been generated to provide a visual overview of the data. The first is a time series plot of the daily price levels. The second is a scatter plot of the daily price change against the previous day's price, which is useful for illustrating whether the magnitude of daily changes is dependent on the price level. If larger daily changes tend to occur at higher price levels, this scatter plot would exhibit a fan-shaped pattern that widens as it moves away from the origin. The third is a time series plot of the daily changes, which allows for the identification of phenomena such as volatility clustering.

Among the four metals, copper holds a particularly significant position. It is the second-most traded non-ferrous metal on the LME and is extensively used in a wide range of industries, including electricity, electronics, construction, energy, architecture, and shipping.

Because of its high industrial demand, the price of copper is closely tied to the global economic cycle. This relationship is often observed as price increases during periods of economic recovery and expansion, and price decreases during economic slowdowns and recessions. As such, copper futures prices, along with oil prices, are widely considered a leading indicator for the real economy. For this reason, copper is affectionately known as "Doctor Copper" in the commodity and economic fields, a nickname that highlights its perceived ability to predict the health of the global economy.

Figure 1 presents three visualizations of the daily LME copper price data. The first panel is a time series plot of the daily copper price over the period from 1987 to 2021. It shows that the copper price remained relatively stable at a low level until around 2005, when it began a steep ascent, driven largely by a surge in demand from China. The price then experienced a sharp decline during the 2008 global financial crisis. Propelled by the subsequent economic recovery, copper prices rose dramatically until 2012, before gradually declining through 2016, influenced by a slowdown in China's economic growth. This pro-cyclical behavior reinforces copper's reputation as a leading economic indicator.

The second panel is a scatter plot of the daily price change against the previous day's price level. The graph illustrates that as the price level increases, the magnitude of daily changes also tends to expand, initially forming a fan-shaped pattern. However, this spread appears to narrow

again when the price exceeds approximately $8,000, suggesting that the volatility of copper prices is not a simple, monotonically increasing function of the price level. The ability to statistically test for the presence of this non-monotonic relationship is a key motivation for employing flexible diffusion models.

The third panel shows the time series plot of the daily price changes. This graph demonstrates the phenomenon of volatility clustering, where periods of high price volatility are followed by similar periods. A dramatic increase in the magnitude of price fluctuations is particularly evident from around 2005, a period that coincides with China's escalating demand and increased speculative capital entering the market.

Among the non-ferrous metals, aluminum is the most traded metal on the LME. This is attributed to its high industrial demand, driven by its lightweight, corrosion resistance, and ease of processing. Aluminum's soft and ductile nature often necessitates alloying with other metals such as copper, manganese, silicon, magnesium, zinc, and nickel to enhance its properties for specific applications. For example, high-strength aluminum alloys are used in the manufacturing of aircraft and car bodies. In 2020, aluminum futures accounted for approximately 42% of the total futures traded on the LME, highlighting its dominant position in the market.

Figure 2 presents three visualizations of the daily LME aluminum price. The top panel displays the time series of the aluminum price from 1993 to 2021. The price remained at a lower level until around 2005, when it began a steep ascent. The price then experienced a sharp decline during the 2008 global financial crisis. Following the crisis, the price continued to fluctuate, but its overall volatility was less pronounced compared to other non-ferrous metals. This relative stability is attributed to aluminum's abundant reserves and a relatively stable global supply. Additionally, its extensive range of applications, from packaging to construction and automotive industries, contributes to a more stable demand, which in turn leads to less extreme price fluctuations than those observed in other metals.

The middle panel is a scatter plot of the daily price change versus the previous day's price. The plot illustrates that the magnitude of daily changes tends to increase as the price level rises. However, the pattern appears to narrow after the price exceeds $2,000, and again after exceeding $3,000, suggesting that the volatility of aluminum prices, like copper, is not a simple, monotonically increasing function of the price level. This

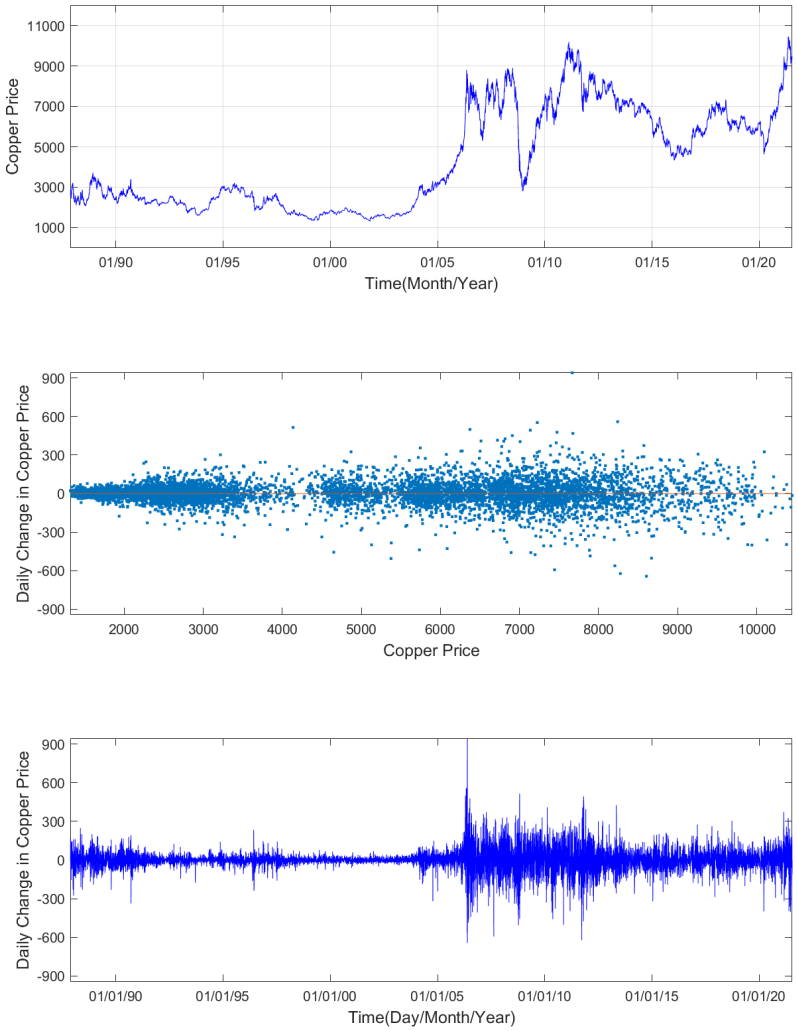

Figure 1: Copper Graphs. Figure 1 displays three graphs of the daily LME copper price data from 1987 to 2021. The first panel is a time series plot of the daily price, the second is a scatter plot of the daily change against the previous day's price, and the third is a time series plot of the daily changes.

non-monotonic relationship motivates the use of flexible diffusion models to capture this complex behavior.

The bottom panel shows the time series of the daily price changes. It provides compelling evidence of volatility clustering, with periods of high price volatility concentrated together. The most extreme volatility is evident around the 2008-2009 financial crisis, highlighting the market's response to major economic events.

Nickel is the fourth most traded metal among the non-ferrous metals on the LME. According to the LME's 'Annual Volume Report', it accounted for approximately 12% of the total futures trading volume on the exchange in 2020. Although the global reserves of nickel are abundant, its refining process is complex and energy-intensive, leading it to be considered a commercially rare metal. Consequently, nickel's price is generally higher compared to copper, aluminum, and zinc. The price of nickel is not only determined by fundamental supply-and-demand dynamics but is also heavily influenced by speculative capital. Recent technological advancements have diversified nickel's applications, bringing it into the spotlight. In particular, nickel has emerged as a crucial raw material for the rapidly growing battery and electric vehicle industries. This has strengthened its link to the automotive market, and its usage is expected to increase substantially in the coming years.

Figure 3 presents three visualizations of the daily LME nickel price data. The first panel displays the time series of the nickel price from 1993 to 2021. The graph shows that the nickel price experienced a steep rise from 2005, followed by a sharp drop during the 2008 global financial crisis. Following this, nickel prices continued to fluctuate, with their movements often corresponding to the stainless steel industry, which historically has accounted for a large portion of nickel demand. More recently, nickel has also become a critical component in electric vehicle battery production, further diversifying its end-uses and making its price highly sensitive to issues and policies related to both the stainless steel and automotive industries.

The second panel is a scatter plot of the daily price change versus the previous day's price. This plot suggests that as the price level increases, the volatility of nickel prices also tends to increase. This heteroskedasticity underscores the need for a diffusion model that can accommodate such a strong dependency.

The third panel shows the time series of the daily price changes.

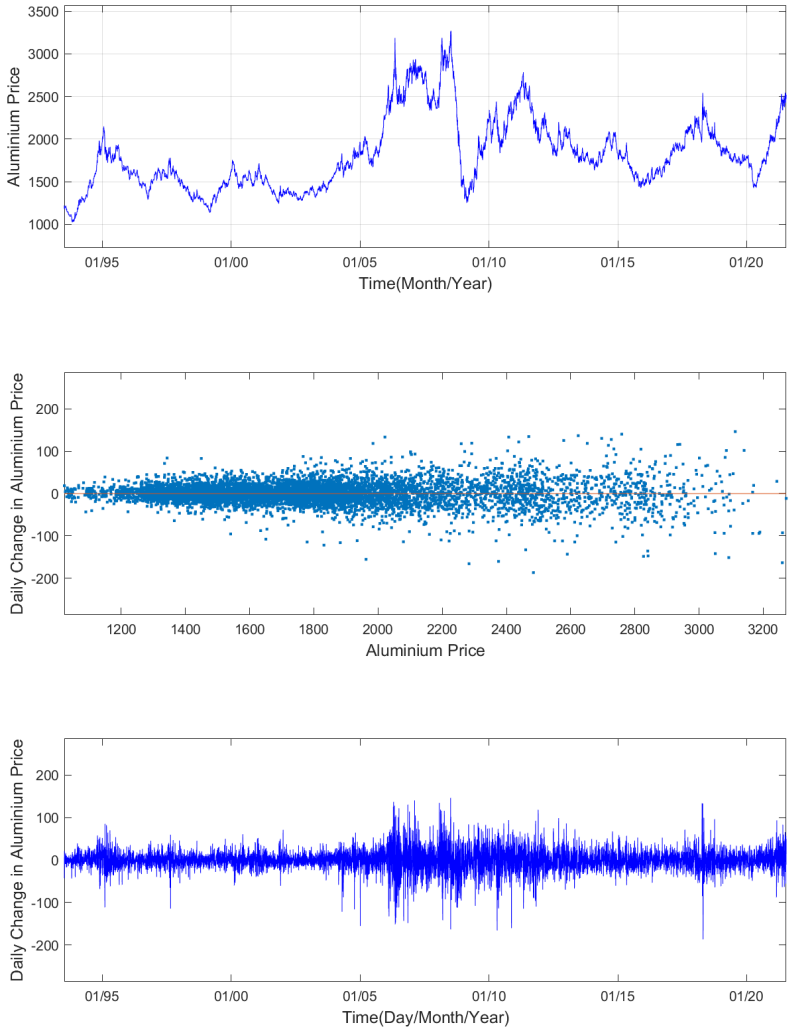

Figure 2: Aluminium Graphs. Figure 2 displays three graphs of the daily LME aluminum price data from 1993 to 2021. The first panel is a time series plot of the daily price, the second is a scatter plot of the daily change against the previous day's price, and the third is a time series plot of the daily changes.

Volatility clustering is evident in this graph, with a distinct period of heightened volatility occurring around 2007-2008. This pronounced volatility clustering, along with the extreme price spike in the time series plot, suggests that nickel price dynamics are particularly complex and likely influenced by non-linear factors and market speculation.

Zinc is the third most traded metal among non-ferrous metals on the LME. According to the LME's 'Annual Volume Report', it accounted for approximately 16% of the total futures trading volume on the exchange in 2020. Zinc is primarily used for galvanization and die-casting of automotive parts. Galvanization, the process of coating steel to prevent corrosion, is particularly sensitive to the construction industry's performance, as it is widely used in steel structures for weather protection. For these reasons, the zinc market is known to be closely related to the global economy. Its price tends to rise during periods of economic expansion and strong construction activity, and fall during periods of economic downturn. This close correlation with global economic health makes zinc a key indicator for industrial activity and a crucial metal to analyze within the non-ferrous group.

Figure 4 presents three visualizations of the daily LME zinc price data. The top panel shows that the zinc price surged from around 2005 before plummeting during the 2008 global financial crisis. The price subsequently experienced another significant increase around 2016, a period attributed to a combination of expectations for a global economic recovery and supply regulations in China due to environmental concerns. This demonstrates that the zinc price is highly sensitive to both demand and supply dynamics. As zinc is closely tied to the construction industry, which is often considered a leading economic indicator, its price also tends to move in sync with the economic cycle. For example, price declines were observed during the 2008 financial crisis and the 2012 Southern European debt crisis.

The middle panel is a scatter plot of the daily price change against the previous day's price. Contrary to a simple fan shape, the plot shows that daily price volatility initially increases with the price level but then appears to decrease at higher price levels. This non-monotonic relationship between price and volatility is a key characteristic that motivates the use of flexible diffusion models.

The bottom panel shows the time series of the daily price changes. This graph demonstrates the phenomenon of volatility clustering, with periods

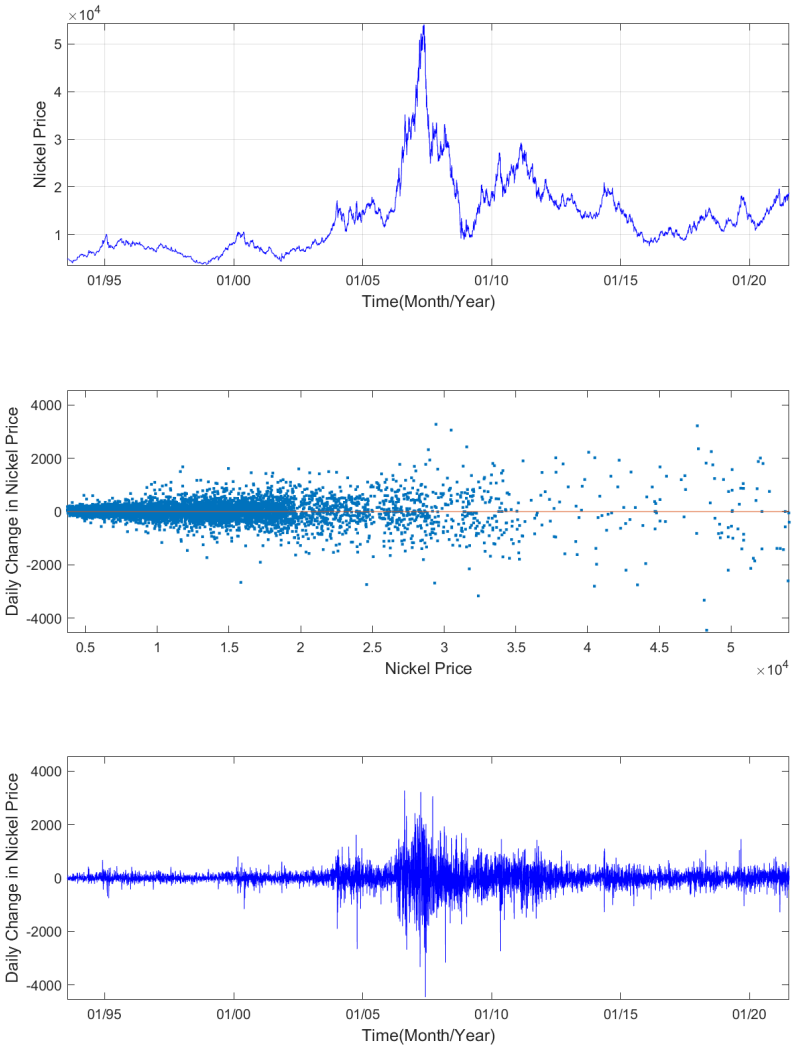

Figure 3: Nickel Graphs. Figure 3 displays three graphs of the daily LME nickel price data from 1993 to 2021. The first panel is a time series plot of the daily price, the second is a scatter plot of the daily change against the previous day's price, and the third is a time series plot of the daily changes.

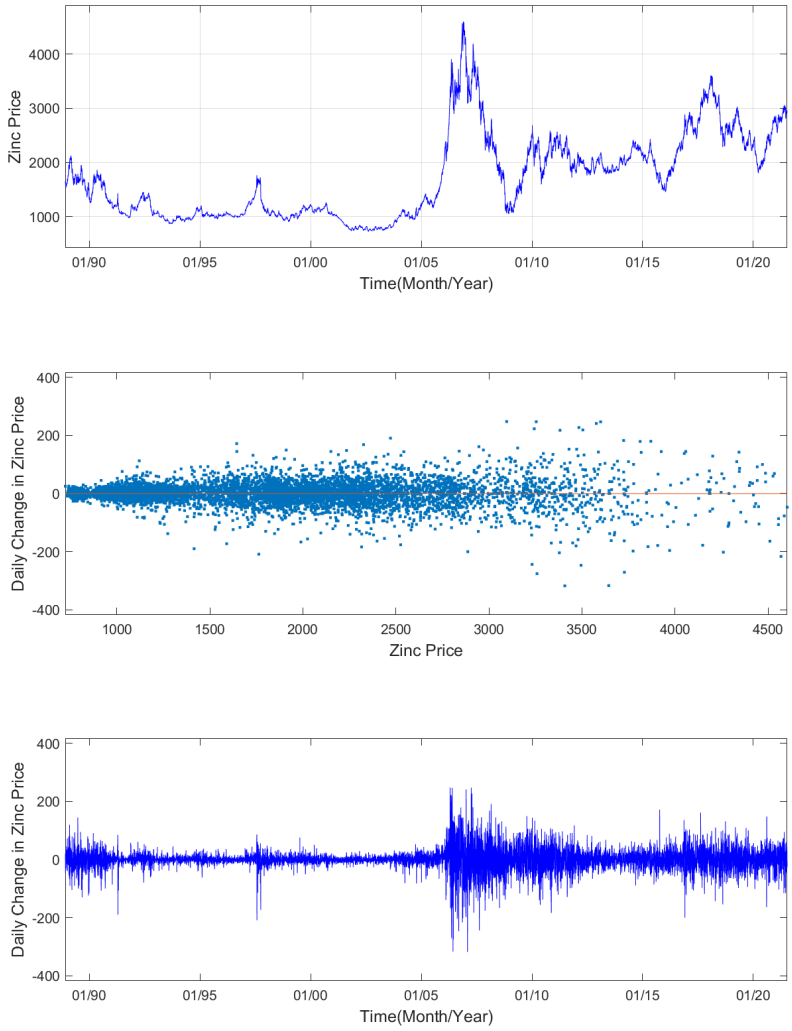

Figure 4: Zinc Graphs. Figure 4 displays three graphs of the daily LME zinc price data from 1988 to 2021. The first panel is a time series plot of the daily price, the second is a scatter plot of the daily change against the previous day's price, and the third is a time series plot of the daily changes.

of high and low volatility grouped together. A period of extremely high volatility is particularly noticeable around the 2007-2008 financial crisis, highlighting the market's reaction to major economic events.

The preliminary visual analysis of the daily price data for copper, aluminum, nickel, and zinc reveals several notable similarities and differences in their dynamic characteristics.

All four metals share a similar long-term price trajectory, with prices remaining relatively low and stable until the mid-2000s. Around 2005, all metals experienced a sharp and sustained price increase, a phenomenon widely attributed to the rapid industrialization and soaring demand from China. This common pattern was followed by a dramatic price collapse during the 2008 global financial crisis, highlighting their collective sensitivity to the global economic cycle.

The scatter plots of daily price changes against price levels for all four metals show clear evidence of heteroskedasticity. The spread of the daily changes generally widens as the price level increases, indicating that price volatility is not constant but is a function of the price level itself. This fan-shaped pattern, though varying in its intensity, is a shared characteristic across all four metals, underscoring the need for diffusion models with non-constant volatility functions.

The time series plots of daily price changes for all metals exhibit distinct periods of volatility clustering. Periods of large price movements (both positive and negative) tend to be followed by similar periods, while calm periods are also clustered together. This behavior is most pronounced during periods of economic turbulence, such as the 2008 financial crisis, suggesting a shared market response to major macroeconomic events.

While all metals show increasing volatility with price, the absolute price levels and the degree of volatility differ significantly. Nickel stands out with a remarkably higher average price and a wider price range between its minimum and maximum values. The scatter plot for nickel shows a more pronounced fan shape, with the price spikes and collapses, suggesting that its volatility is more extreme and highly sensitive to price levels compared to the other metals.

Although all four are sensitive to the global economy, the specific drivers differ. Copper is often seen as a leading economic indicator due to its widespread use in construction and electronics. Zinc is also closely tied to construction through its use in galvanization. Nickel, while historically linked to the stainless steel industry, has seen its price dynamics increasingly influenced by the high-tech and electric vehicle battery sectors, making it more susceptible to speculative capital and specific techno-

logical advancements. Aluminum, with its abundant reserves and stable supply, tends to exhibit less extreme volatility compared to the others.

While all scatter plots show a general trend of increasing volatility with price, the exact relationship is not identical. The fan-shaped pattern for copper and aluminum, as noted previously, appears to narrow at very high price levels, suggesting a non-monotonic relationship. In contrast, nickel's fan shape is more consistently and dramatically widening, particularly at its highest price levels. This indicates that a simple, single volatility function might not be sufficient to capture the nuanced behavior of all four metals, necessitating the use of flexible models that can accommodate these subtle differences.

3. DIFFUSION MODELS AND ESTIMATION METHOD

3.1. DIFFUSION MODELS

In this study, five univariate time-homogeneous diffusion processes are estimated for each of the four metal prices to explain their movements. The maximum likelihood estimation method is used. For the sake of estimation convenience, the prices of copper, aluminum, and nickel were converted to prices per 0.1 kg, while the price of zinc was converted to the price per 1 kg.

The general form of the diffusion model is in equation (1).

$$dX_t = \mu(X_t;\theta)\,dt + \sigma(X_t;\theta)\,dW_t. \tag{1}$$

Here, W_t is a standard Brownian Motion, $\mu(X_t;\theta)$ is a drift function, and $\sigma(X_t;\theta)$ is a volatility function. A variety of diffusion models have been proposed in previous studies.

Table 2 summarizes the mathematical form of each model we employ. The most comprehensive model is the General Drift and General Volatility (GD-GV) model suggested by Choi (2009). This model is highly flexible and encompasses almost all other diffusion models proposed in the literature. The General Drift and Constant Elasticity of Variance (GD-CEV) model is a restricted version of the GD-GV model, where the volatility function is simplified to the Constant Elasticity of Variance (CEV) form. However, its drift function remains highly flexible. The Chan-Karolyi-Longstaff-Sanders (CKLS) model, proposed in Chan *et al.* (1992), is a more restricted model with a linear drift function and a CEV volatility function. The Cox–Ingersoll–Ross (CIR) model, introduced in Cox *et al.*

Model	**Equation**
Vasicek	$dX_t = (\alpha_0 + \alpha_1 X_t)\,dt + \sqrt{\beta_2}\,dW_t$
CIR	$dX_t = (\alpha_0 + \alpha_1 X_t)\,dt + \sqrt{\beta_2 X_t}\,dW_t$
CKLS	$dX_t = (\alpha_0 + \alpha_1 X_t)\,dt + \sqrt{\beta_2 X_t^{\beta_3}}\,dW_t$
GD-CEV	$dX_t = \left(\alpha_{-1} X_t^{-1} + \alpha_0 + \alpha_1 X_t + \alpha_2 X_t^2 + \alpha_3 X_t^3\right) dt + \sqrt{\beta_2 X_t^{\beta_3}}\,dW_t$
GD-GV	$dX_t = \left(\alpha_{-1} X_t^{-1} + \alpha_0 + \alpha_1 X_t + \alpha_2 X_t^2 + \alpha_3 X_t^3\right) dt + \sqrt{\beta_0 + \beta_1 X_t + \beta_2 X_t^{\beta_3}}\,dW_t$

Table 2: Diffusion Models for Metal Prices. This table summarizes the five diffusion models used in this study, which include the Vasicek, CIR, CKLS, GD-CEV, and GD-GV models.

(1985), is a special case of the CKLS model where the elasticity parameter β_3 is restricted to 1. It features a linear drift and a volatility that is proportional to the square root of the price. Finally, the Vasicek model, from Vasicek (1977), is characterized by a linear drift function and a constant volatility.

The models are nested in the following relationship. Vasicek and CIR are special cases of CKLS, which in turn is a special case of GD-CEV. All four of these models are nested within the most general GD-GV model. This hierarchical structure allows for a robust comparison of models, from the simplest to the most complex, to determine which one provides the most appropriate representation of the data.

3.2. MAXIMUM LIKELIHOOD ESTIMATION

We employ the maximum likelihood estimation (MLE) method to estimate the diffusion models. If the transition probability density function (TPDF) of a diffusion model is known, the log-joint probability density function of the daily metal prices can be written as follows, ignoring the first observation.

$$l_n(\theta) = \sum_{i=1}^{n} \ln\left[p_X(\Delta, X_{i\Delta} \mid X_{(i-1)\Delta}; \theta)\right], \tag{2}$$

where $p_X(\Delta, X_{i\Delta} \mid X_{(i-1)\Delta}; \theta)$ is the TPDF of a diffusion process at time $i\Delta$ given $X_{(i-1)\Delta}$. We observe metal prices X_t discretely at times $t =$

$i\Delta$, $i = 0, 1, \ldots, n$, where Δ is the time difference between two consecutive observations and $\Delta = \frac{1}{252}$ in the case of daily data.

However, to apply the MLE and ensure the efficiency of its estimators, we must know the TPDF of the diffusion process. While the TPDF is known for a few diffusion models such as Vasicek (1977), CIR (1985), and Black and Scholes (1973), it is unknown for most diffusion process models. Therefore, we first obtain an approximate yet accurate log-TPDF in a closed form using the method developed by (Aït-Sahalia, 2008) [2]. Then we use it to estimate the parameters via the Maximum Likelihood Estimation method.

In a groundbreaking work, Aït-Sahalia (2008) conjectured that even for an irreducible diffusion process, the log-TPDF retains the same form as that of a reducible model. Accordingly, even in the irreducible case, the log-TPDF can be expressed as in equation (3).

$$\begin{aligned} l_X^{(K)}(\Delta, x \mid x_0; \theta) = &-\tfrac{1}{2}\ln(2\pi\Delta) - D_v(x;\theta) + \frac{C_X^{(-1)}(\Delta, x \mid x_0; \theta)}{\Delta} \\ &+ \sum_{k=0}^{K} C_X^{(k)}(\Delta, x \mid x_0; \theta)\frac{\Delta^k}{k!}\,. \end{aligned} \tag{3}$$

The subsequent process can be summarized as follows. First, substitute equation (3) into the following Kolmogorov partial differential equations.

$$\begin{aligned} \frac{\partial l_X(\Delta, x \mid x_0; \theta)}{\partial \Delta} = &-\frac{\partial \mu_i(x;\theta)}{\partial x_i} + \frac{1}{2}\frac{\partial^2 v_{ij}(x;\theta)}{\partial x_i \partial x_j} \\ &- \mu_i(t,x)\,\frac{\partial l_X(\Delta, x \mid x_0; \theta)}{\partial x_i} \\ &+ \frac{\partial v_{ij}(x;\theta)}{\partial x_i}\,\frac{\partial l_X(\Delta, x \mid x_0)}{\partial x_j} \\ &+ \tfrac{1}{2} v_{ij}(x;\theta)\,\frac{\partial^2 l_X(\Delta, x \mid x_0; \theta)}{\partial x_i \partial x_j} \\ &+ \tfrac{1}{2}\frac{\partial l_X(\Delta, x \mid x_0)}{\partial x_i}\, v_{ij}(x;\theta)\,\frac{\partial l_X(\Delta, x \mid x_0)}{\partial x_j}. \end{aligned} \tag{4}$$

[2] A more detailed explanation of the methods for obtaining the approximate TPDF, ranging from Aït-Sahalia's univariate time-homogeneous diffusion model (Aït-Sahalia, 2002) to Choi's multivariate time-inhomogeneous diffusion model (Choi, 2015a), is well-summarized in (Choi, 2020a).

Secondly, by comparing terms of the same order of Δ, we derive the partial differential equations (PDEs) that each coefficient $C_X^{(k)}(\Delta, x \mid x_0; \theta)$, $(k = -1, 0, \ldots, K)$ satisfies. The approximate log-TPDF can be obtained by solving these PDEs. While these PDEs can be solved for reducible diffusion models, they cannot be solved for irreducible models. For this reason, Aït-Sahalia (2008) suggests that in the PDEs of each coefficient, $C_X^{(k)}(\Delta, x \mid x_0; \theta)$ and all other functions of x are Taylor expanded around the value x_0. Next, by comparing terms of the same order of $(x - x_0)$ in these Taylor series expansions, the Taylor series of $C_X^{(k)}(\Delta, x \mid x_0; \theta)$ can be obtained up to the desired order. By substituting $C_X^{(j_k,k)}(\Delta, x \mid x_0; \theta)$, which represents the Taylor series of $C_X^{(k)}(\Delta, x \mid x_0; \theta)$ up to the j_k order, into equation (3), we can obtain the approximate log-TPDF as follows[3]

$$\tilde{l}_X^{(K)}(\Delta, x \mid x_0; \theta) = -\tfrac{1}{2}\ln(2\pi\Delta) - D_v(x; \theta) + \frac{C_X^{(j_{-1},-1)}(\Delta, x \mid x_0; \theta)}{\Delta} + \sum_{k=0}^{K} C_X^{(j_k,k)}(\Delta, x \mid x_0; \theta)\frac{\Delta^k}{k!}. \tag{5}$$

Finally, by substituting equation (5) into the combined equation (2), we can obtain the maximum likelihood estimate.

4. ESTIMATION RESULTS AND DISCUSSIONS

Five diffusion models—Vasicek, CIR, CKLS, GD-CEV, and GD-GV—are applied to four non-ferrous metal prices. The most suitable model is determined using the Akaike information criterion (Akaike, 1973), the Bayesian information criterion (Schwarz, 1978), and the likelihood ratio test.

The Akaike information criterion (AIC) is defined as $\mathrm{AIC} = 2k - 2\ln(\hat{L})$, where k is the number of parameters being estimated and $\hat{L}$ is the estimated maximum likelihood. Akaike (1973) shows that it can be viewed as the estimator of the information loss associated with the corresponding model. Therefore, we prefer the model that gives the least value of AIC. The Bayesian information criterion (BIC) is defined as $\mathrm{BIC} = k\ln(n) - 2\ln(\hat{L})$, where k is the number of parameters being estimated, $\hat{L}$ is the estimated maximum likelihood, and n is the number of

[3]During the calculation of the coefficients, each coefficient depends on the lower-order coefficients. Therefore, they must be derived sequentially, starting from $K = -1$, and the Taylor expansion must be obtained from the lowest order first. In this study, we used the approximate log-TPDF up to the $K = 1$ order.

observations. Like AIC, it measures the information loss, but by adding the $k\ln(n)$ term, it imposes a greater penalty on the model as the number of parameters increases. If two models give the equal likelihood value, BIC will prefer the parsimonious model.

4.1. ESTIMATION RESULTS FOR COPPER

We applied five diffusion models—Vasicek, CIR, CKLS, GD-CEV, and GD-GV—to the daily LME copper price data to identify the model that best explains its dynamics. The estimation results are summarized in Table 3, with the estimated drift and volatility functions presented in Figure 5.

Based on the estimation results, the CKLS model is the most appropriate for describing the dynamics of copper prices. When the CKLS model was tested against the more general GD-GV model using the likelihood ratio test, the p-value was 0.07. This means that at a 5% significance level, the CKLS model cannot be rejected in favor of the more complex GD-GV model. Additionally, the AIC is smallest for the GD-CEV model, while the BIC is smallest for the CKLS model. Given the statistical insignificance of the additional parameters in the GD-GV model, and the inability to reject the CKLS model at the 5% level, the CKLS model provides the most parsimonious and suitable fit for the copper price data.

Upon examining the estimated parameters, it is notable that the drift parameters $(\alpha_{-1}, \alpha_0, \alpha_1, \alpha_2, \alpha_3)$ for all models are statistically insignificant at the 5% level. This is visually confirmed in the drift function graphs of Figure 5, where the 95% confidence bands for most models include the x-axis for the entire range of observed prices. However, a closer look at the GD-CEV and GD-GV drift functions reveals some evidence of a mean-reverting property, as their 95% confidence bands are slightly above the x-axis in the price range around 0.5. This suggests that while not statistically strong, there is a tendency for the price to revert to its mean in certain middle-price scenarios.

In contrast, the volatility parameters (β_2, β_3) for all non-Vasicek models are highly significant at the 1% level. This finding indicates that the volatility of copper prices is strongly dependent on the price level. The volatility function graphs in Figure 5 further support this, showing that volatility is an increasing function of the copper price. The GD-CEV model shows a volatility function that increases with the price at a rate determined by the significant β_3 parameter, confirming the heteroskedas-

θ	Vasicek	CIR	CKLS	GD–CEV	GD–GV
Panel A. Drift parameters					
α_{-1}	0	0	0	0.065	0.065
(std.err)				(0.042)	(0.042)
α_0	0.026	0.017	0.013	-0.71	-0.71
(std.err)	(0.037)	(0.021)	(0.013)	(0.54)	(0.54)
α_1	-0.016	-0.00	-0.00	2.29	2.29
(std.err)	(0.055)	(0.042)	(0.046)	(2.30)	(2.32)
α_2	0	0	0	-1.91	-1.91
(std.err)				(3.90)	(3.93)
α_3	0	0	0	-0.00	-0.00
(std.err)				(2.25)	(2.26)
Panel B. Volatility parameters					
β_0	0	0	0	0	0.00
(std.err)					(0.00020)
β_1	0	0	0	0	0
(std.err)					(0.0024)
β_2	0.0080^{**}	0.015^{**}	0.041^{**}	0.040^{**}	0.040^{**}
(std.err)	(0.000027)	(0.000057)	(0.00041)	(0.00040)	(0.0017)
β_3	0	1	2.16^{**}	2.16^{**}	2.14^{**}
(std.err)			(0.0090)	(0.0090)	(0.11)
Panel C. Criterions					
log-lik	49368.91	53066.12	54657.73	54661.27	54661.27
LR test (p-val)	0	0	0.21	1	–
AIC	-98731.82	-106126.24	-109307.46	-109308.54	-109304.54
BIC	-98710.58	-106105.00	-109279.14	-109258.98	-109240.82

Table 3: Estimation Results for Copper. ** indicates statistical significance at the 1% level. * indicates statistical significance at the 5% level. The numbers in parentheses below the estimated values are the standard errors of the parameters. The table presents maximum likelihood estimation results for five diffusion models applied to daily LME copper prices. It is organized into three panels: Panel A for drift parameters, Panel B for volatility parameters, and Panel C for information criteria and the likelihood ratio (LR) test.

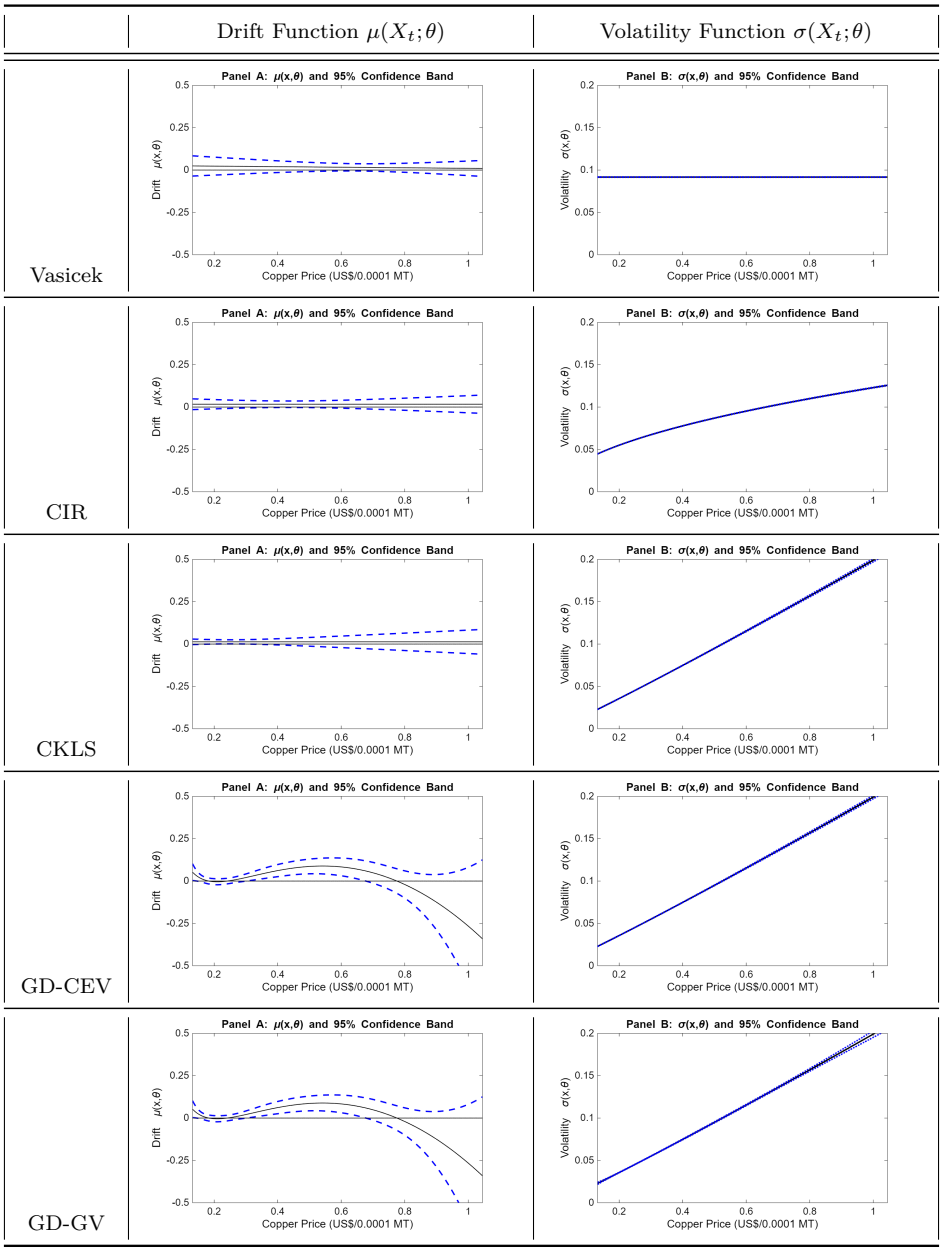

Figure 5: Drift and Volatility Functions for Copper. The drift and volatility functions were evaluated using the estimated parameters from each diffusion model over the range of observed copper prices. The dashed lines represent the 95% confidence bands for the estimated functions.

ticity observed in the preliminary visual analysis. The elasticity of volatility with respect to the price, given by $\beta_3/2$ in the CEV-type models, is estimated to be approximately 1.08, suggesting that a 1% increase in the copper price leads to a more than 1% increase in its volatility.

Overall, the estimation results for copper suggest that its price dynamics are best described by a model with a CEV volatility structure, but a statistically insignificant drift term. This highlights that for copper, volatility is a more critical component than mean-reversion in explaining its price movements.

4.2. ESTIMATION RESULTS FOR ALUMINUM

We estimated five diffusion models—Vasicek, CIR, CKLS, GD-CEV, and GD-GV—using daily LME aluminum price data to capture its underlying dynamics. The key findings of this analysis are presented in the summary statistics of Table 4 and visualized through the estimated drift and volatility functions in Figure 6.

The empirical results for aluminum reveal distinct characteristics compared to copper. When comparing the five models, the GD-GV and GD-CEV models exhibit a strong performance with high log-likelihood values. However, the likelihood ratio test results are mixed. While both the CKLS and GD-CEV models are rejected against the GD-GV model, the information criteria present a divided picture. The AIC is lowest for the GD-GV model, which suggests that its additional parameters are valuable for capturing the data's dynamics. Conversely, the BIC, which applies a heavier penalty for the number of parameters, favors the simpler CKLS model. This conflicting evidence suggests that either the GD-GV or the CKLS model could be considered the most appropriate for explaining aluminum price movements, depending on the chosen criterion.

In terms of mean reversion, the simpler models (Vasicek, CIR, and CKLS) show statistically significant drift parameters (α_0, α_1), providing some evidence that aluminum prices tend to revert to a long-run mean. This is graphically confirmed in Figure 6, where the 95% confidence bands of their drift functions lie consistently above the x-axis. However, since the drift function remains close to the x-axis, the strength of this mean reversion does not appear to be very large. Furthermore, this statistically significant result is not found in the more general GD-CEV and GD-GV models with their more flexible drift terms.

The role of volatility is equally important. All models show highly sig-

nificant volatility parameters. Notably, the GD-GV model, which proved to be the best fit, provides a more complex picture. As seen in the volatility function graphs in Figure 6, volatility is a monotonically increasing function of the aluminum price. The estimated elasticity of volatility with respect to price, approximately 1.60, was calculated based on the similar β_3 estimates from both the GD-CEV and GD-GV models. This indicates that aluminum's price fluctuations are highly responsive to changes in its price level.

To summarize, the GD-GV and CKLS models emerge as the most plausible candidates for describing aluminum prices, though a definitive conclusion depends on the model selection criteria used. While the mean-reverting property is statistically significant in simpler models, the general volatility function is essential for capturing the complete dynamics, as evidenced by the significance of its additional parameters. This suggests that a more complex model is required to fully understand the behavior of aluminum prices.

4.3. ESTIMATION RESULTS FOR NICKEL

We estimated five diffusion models—Vasicek, CIR, CKLS, GD-CEV, and GD-GV—to analyze the dynamic behavior of daily LME nickel prices. The key findings from this analysis are presented in Table 5, and the estimated drift and volatility functions are visualized in Figure 7.

The empirical results for nickel reveal a pattern distinct from the other non-ferrous metals. A statistical comparison using log-likelihood values and information criteria indicates that the CKLS model is the most suitable for describing nickel's price dynamics. When the CKLS and GD–CEV models are tested against the more general GD-GV model, both are not rejected, suggesting that the additional parameters in the GD-GV model are statistically insignificant. Furthermore, when the CKLS model is tested against the GD-CEV model, the p-value is 0.96, meaning that at any conventional significance level, the CKLS model cannot be rejected in favor of the more general GD-CEV model. Both the AIC and BIC values are also smallest for the CKLS model. This strong evidence suggests that the CKLS model is the most appropriate choice for explaining the price movements of nickel.

When we examine the drift component, the linear drift models (Vasicek and CIR) show a drift function that is close to the x-axis, suggesting that while there may be a tendency towards mean reversion, the effect is

θ	Vasicek	CIR	CKLS	GD–CEV	GD–GV
Panel A. Drift parameters					
α_{-1}	0	0	0	0.00010	0.0056
(std.err)				(0.10)	(0.12)
α_0	0.045^{**}	0.044^{**}	0.034^{*}	0.16	0.082
(std.err)	(0.017)	(0.016)	(0.014)	(2.40)	(2.76)
α_1	-0.22^{**}	-0.22^{**}	-0.16	-2.48	-2.22
(std.err)	(0.078)	(0.079)	(0.088)	(20.85)	(23.58)
α_2	0	0	0	13.72	14.021
(std.err)				(77.89)	(87.11)
α_3	0	0	0	-25.83	-27.65
(std.err)				(105.63)	(117.12)
Panel B. Volatility parameters					
β_0	0	0	0	0	0.00041^{**}
(std.err)					(0.00012)
β_1	0	0	0	0	-0.0039^{*}
(std.err)					(0.0016)
β_2	0.00081^{**}	0.0040^{**}	0.17^{**}	0.17^{**}	0.18^{**}
(std.err)	(0.00)	(0.000019)	(0.0075)	(0.0076)	(0.039)
β_3	0	1	3.27^{**}	3.27^{**}	3.085^{**}
(std.err)			(0.025)	(0.025)	(0.23)
Panel C. Criterions					
log-lik	58148.16	59233.65	60233.01	60233.31	60245.25
LR test (p-val)	0	0	0	0	–
AIC	-116290.32	-118461.30	-120458.02	-120452.62	-120472.50
BIC	-116269.63	-118440.61	-120430.43	-120404.35	-120410.43

Table 4: Estimation Results for Aluminum. ** indicates statistical significance at the 1% level. * indicates statistical significance at the 5% level. The numbers in parentheses below the estimated values are the standard errors of the parameters. The table presents maximum likelihood estimation results for five diffusion models applied to daily LME aluminum prices. It is organized into three panels: Panel A for drift parameters, Panel B for volatility parameters, and Panel C for information criteria and the likelihood ratio (LR) test.

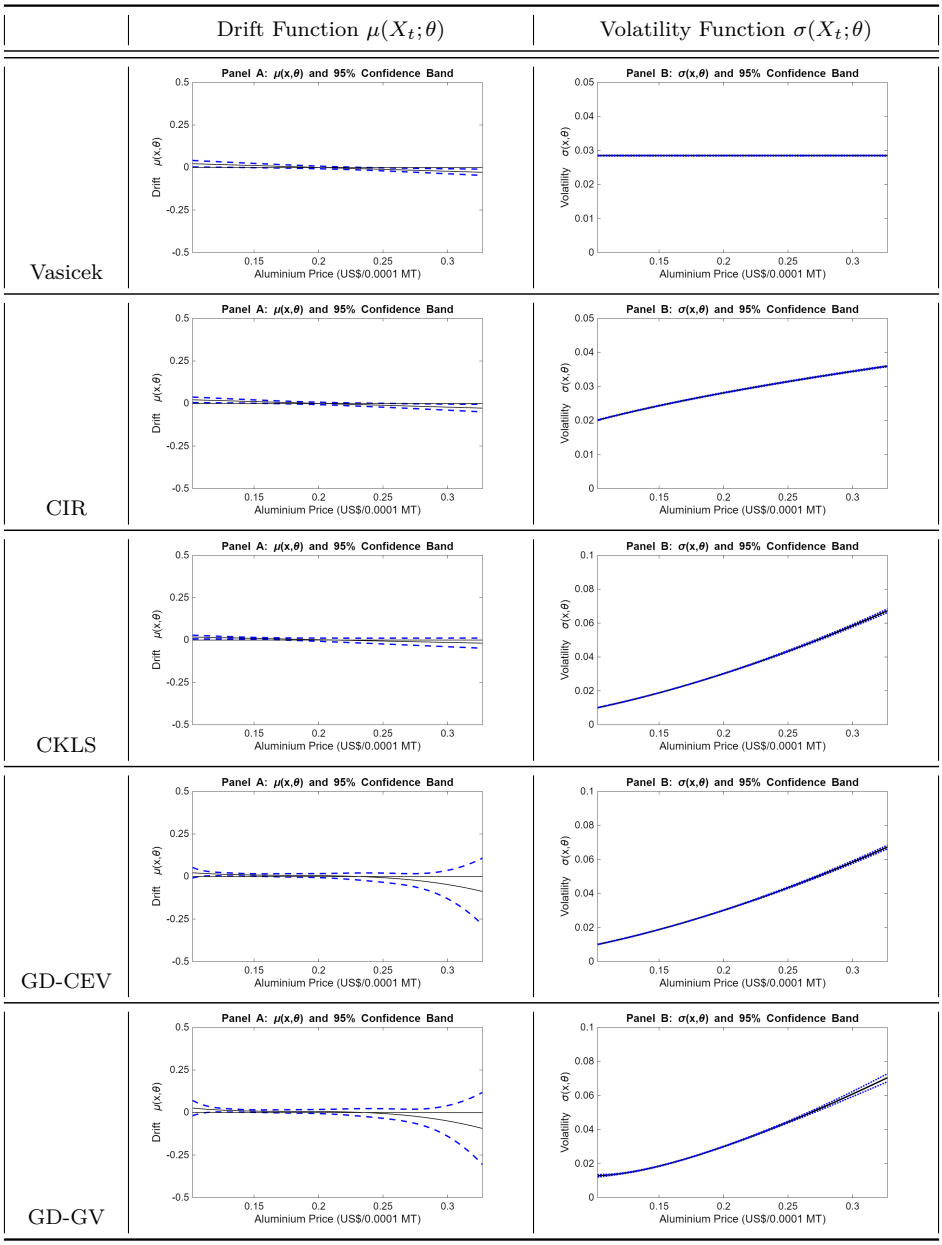

Figure 6: Drift and Volatility Functions for Aluminum. The drift and volatility functions were evaluated using the estimated parameters from each diffusion model over the range of observed aluminum prices. The dashed lines represent the 95% confidence bands for the estimated functions.

not strong. This is also visually confirmed in Figure 7, where the 95% confidence bands for these models lie consistently away from the x-axis, but closely to it. However, the more flexible GD-CEV and GD-GV models fail to produce statistically significant drift parameters, with their confidence bands almost entirely overlapping the x-axis. This suggests that while a simple linear relationship might indicate mean reversion, a more nuanced, non-linear perspective does not provide statistically significant evidence for it.

The volatility component, in contrast, consistently demonstrates strong statistical significance across all models. The volatility parameters for all models are highly significant at the 1% level. As seen in the volatility function graphs in Figure 7, nickel's volatility is a monotonically increasing function of its price. The elasticity of volatility with respect to price, calculated from the similar β_3 estimates of the CKLS, GD-CEV, and GD-GV models, is approximately 1.19. This suggests that a 1% increase in the nickel price leads to a corresponding 1.19% increase in its volatility, a responsiveness that reflects the metal's high susceptibility to market forces.

To summarize, the price dynamics of nickel are best captured by a model with a flexible volatility structure, such as the CKLS model. While the drift component shows some evidence of mean reversion in simpler models, this finding is not robust when more complex, general models are used. This highlights that volatility is the dominant factor in explaining nickel price movements.

4.4. ESTIMATION RESULTS FOR ZINC

We estimated five diffusion models—Vasicek, CIR, CKLS, GD-CEV, and GD-GV—to analyze the dynamic behavior of daily LME zinc prices. The key findings from this analysis are presented in Table 6, and the estimated drift and volatility functions are visualized in Figure 8.

The empirical results for zinc reveal a pattern that, while sharing some similarities, has its own unique characteristics. A statistical comparison using log-likelihood values and information criteria indicates that the CKLS, GD-CEV, and GD-GV models are the most suitable for describing zinc's price dynamics. When the CKLS and GD-CEV models are tested against the more general GD-GV model, both are not rejected, suggesting that the additional parameters in the GD-GV model are statistically insignificant. Furthermore, when the CKLS model is tested against the

θ	Vasicek	CIR	CKLS	GD–CEV	GD–GV
Panel A. Drift parameters					
α_{-1}	0	0	0	0.00010	0.00010
(std.err)				(0.25)	(0.26)
α_0	0.26^{*}	0.22^{*}	0.098	0.099	0.089
(std.err)	(0.13)	(0.093)	(0.056)	(1.013)	(1.028)
α_1	-0.16^{**}	-0.13^{*}	-0.020	-0.015	-0.041
(std.err)	(0.044)	(0.053)	(0.068)	(1.30)	(1.31)
α_2	0	0	0	0.0061	0.067
(std.err)				(0.61)	(0.62)
α_3	0	0	0	-0.0083	-0.026
(std.err)				(0.090)	(0.091)
Panel B. Volatility parameters					
β_0	0	0	0	0	0.00020
(std.err)					(0.0016)
β_1	0	0	0	0	0.00010
(std.err)					(0.0053)
β_2	0.17^{**}	0.085^{**}	0.052^{**}	0.052^{**}	0.052^{**}
(std.err)	(0.00049)	(0.00034)	(0.00025)	(0.00025)	(0.0037)
β_3	0	1	2.38^{**}	2.38^{**}	2.38^{**}
(std.err)			(0.0097)	(0.0098)	(0.056)
Panel C. Criterions					
log-lik	19036.83	23109.86	25182.98	25183.13	25183.97
LR test	0	0	0.85	0.43	–
(p-val)	0	0	0	0	
AIC	-38067.66	-46213.72	-50357.96	-50352.26	-50349.94
BIC	-38046.97	-46193.03	-50330.38	-50303.99	-50287.88

Table 5: Estimation Results for Nickel. ** indicates statistical significance at the 1% level. * indicates statistical significance at the 5% level. The numbers in parentheses below the estimated values are the standard errors of the parameters. The table presents maximum likelihood estimation results for five diffusion models applied to daily LME nickel prices. It is organized into three panels: Panel A for drift parameters, Panel B for volatility parameters, and Panel C for information criteria and the likelihood ratio (LR) test.

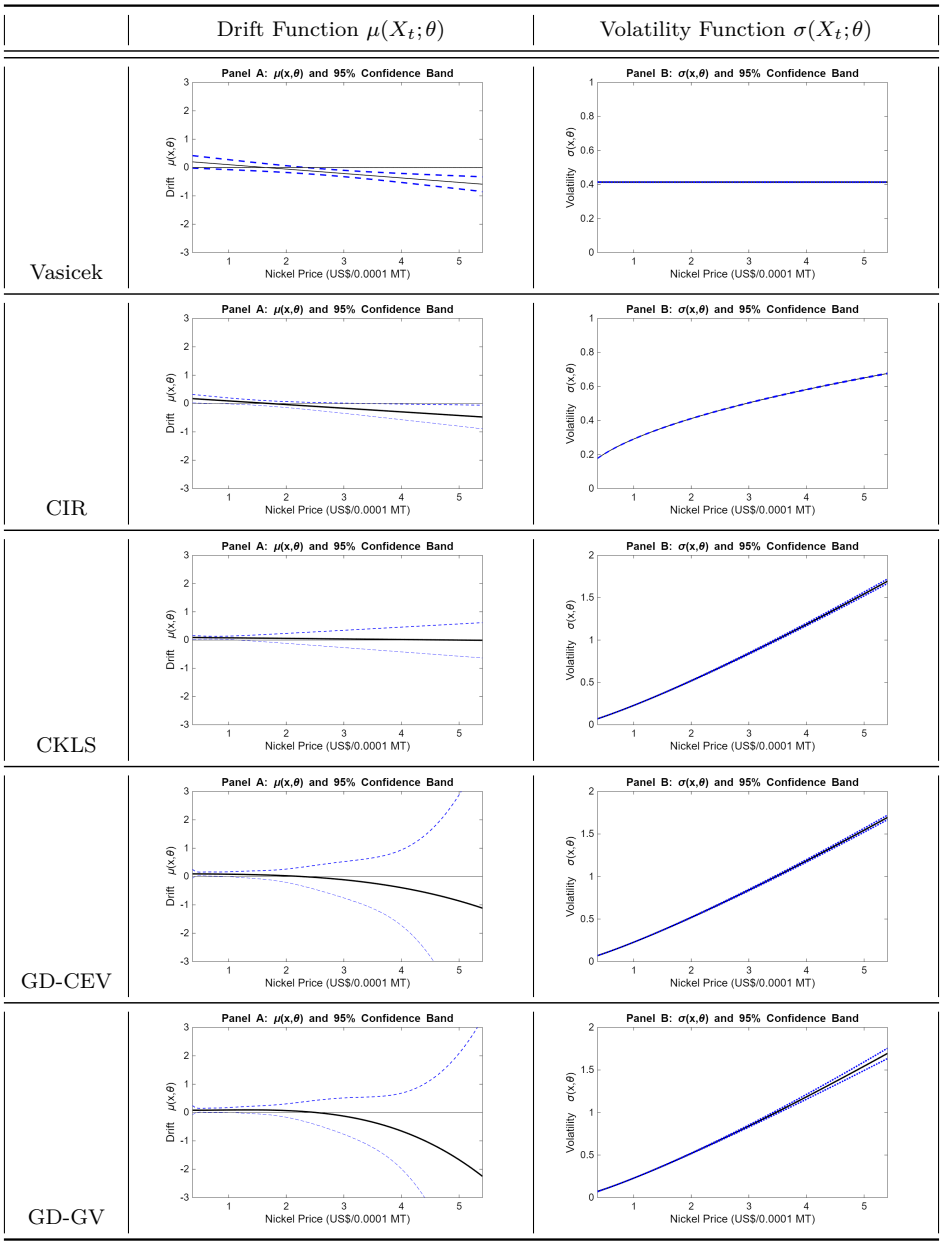

Figure 7: Drift and Volatility Functions for Nickel. The drift and volatility functions were evaluated using the estimated parameters from each diffusion model over the range of observed nickel prices. The dashed lines represent the 95% confidence bands for the estimated functions.

GD-CEV model, the p-value is 0.40, meaning that at any conventional significance level, the CKLS model cannot be rejected in favor of the more general GD-CEV model. Both the AIC and BIC values are also smallest for the CKLS model, making it the most parsimonious and appropriate choice. This suggests that the additional drift parameters in the GD-CEV and GD-GV models are not statistically significant for explaining zinc's price movements.

When we examine the drift component, the drift parameters for all models are not statistically significant at any conventional level. This is visually confirmed in Figure 8, where the 95% confidence bands for all models lie consistently encompassing the x-axis for the entire range of observed prices. This suggests that there is no statistically significant evidence of a mean-reverting property in the zinc price data.

The volatility component, in contrast, consistently demonstrates strong statistical significance across all models. The volatility parameters for all models are highly significant at the 1% level. As seen in the volatility function graphs in Figure 8, zinc's volatility is a monotonically increasing function of its price. The elasticity of volatility with respect to price, calculated from the similar β_3 estimates of the CKLS, GD-CEV, and GD-GV models, is approximately 1.42. This suggests that a 1% increase in the zinc price leads to a corresponding 1.42% increase in its volatility.

To summarize, the price dynamics of zinc are best captured by a model with a flexible volatility structure, such as the CKLS model. The drift component, however, does not show statistically significant evidence of a mean-reverting property in the zinc price data. This highlights that volatility is the dominant factor in explaining zinc price movements.

4.5. COMPARISON AND DISCUSSION

The estimation results for the four non-ferrous metals reveal both shared characteristics and distinct differences in their price dynamics. All four metals consistently show that price volatility is a dominant factor, with volatility functions monotonically increasing with price level, a clear indication of heteroskedasticity. However, the selection of the most appropriate model and the significance of the drift component vary. For aluminum, the complex GD-GV model emerged as the best fit, as the likelihood ratio test rejected all simpler nested models, suggesting that its unique dynamics require a more generalized framework. In contrast, for copper, nickel, and zinc, the simpler CKLS model was identified as

θ	Vasicek	CIR	CKLS	GD–CEV	GD–GV
Panel A. Drift parameters					
α_{-1}	0	0	0	1.090	1.090
(std.err)				(1.59)	(1.59)
α_0	0.21	0.17	0.053	-2.19	-2.18
(std.err)	(0.16)	(0.12)	(0.085)	(4.43)	(4.43)
α_1	-0.099	-0.075	-0.00052	1.22	1.22
(std.err)	(0.058)	(0.057)	(0.069)	(4.29)	(4.29)
α_2	0	0	0	-0.056	-0.056
(std.err)				(1.69)	(1.69)
α_3	0	0	0	-0.052	-0.052
(std.err)				(0.23)	(0.23)
Panel B. Volatility parameters					
β_0	0	0	0	0	0.00
(std.err)					(0.0038)
β_1	0	0	0	0	-0.00016
(std.err)					(0.0068)
β_2	0.16^{**}	0.071^{**}	0.024^{**}	0.024^{**}	0.024^{**}
(std.err)	(0.00053)	(0.0003)	(0.00016)	(0.00016)	(0.0030)
β_3	0	1	2.84^{**}	2.84^{**}	2.84^{**}
(std.err)			(0.014)	(0.014)	(0.093)
Panel C. Criterions					
log-lik	22820.30	25961.36	28282.85	28284.33	28285.86
LR test	0	0	0.30	0.22	–
(p-val)	0	0	0	0	
AIC	-45634.60	-51916.72	-56557.70	-56554.66	-56553.72
BIC	-45613.45	-51895.57	-56529.50	-56505.32	-56490.28

Table 6: Estimation Results for Zinc. ** indicates statistical significance at the 1% level. * indicates statistical significance at the 5% level. The numbers in parentheses below the estimated values are the standard errors of the parameters. The table presents maximum likelihood estimation results for five diffusion models applied to daily LME zinc prices. It is organized into three panels: Panel A for drift parameters, Panel B for volatility parameters, and Panel C for information criteria and the likelihood ratio (LR) test.

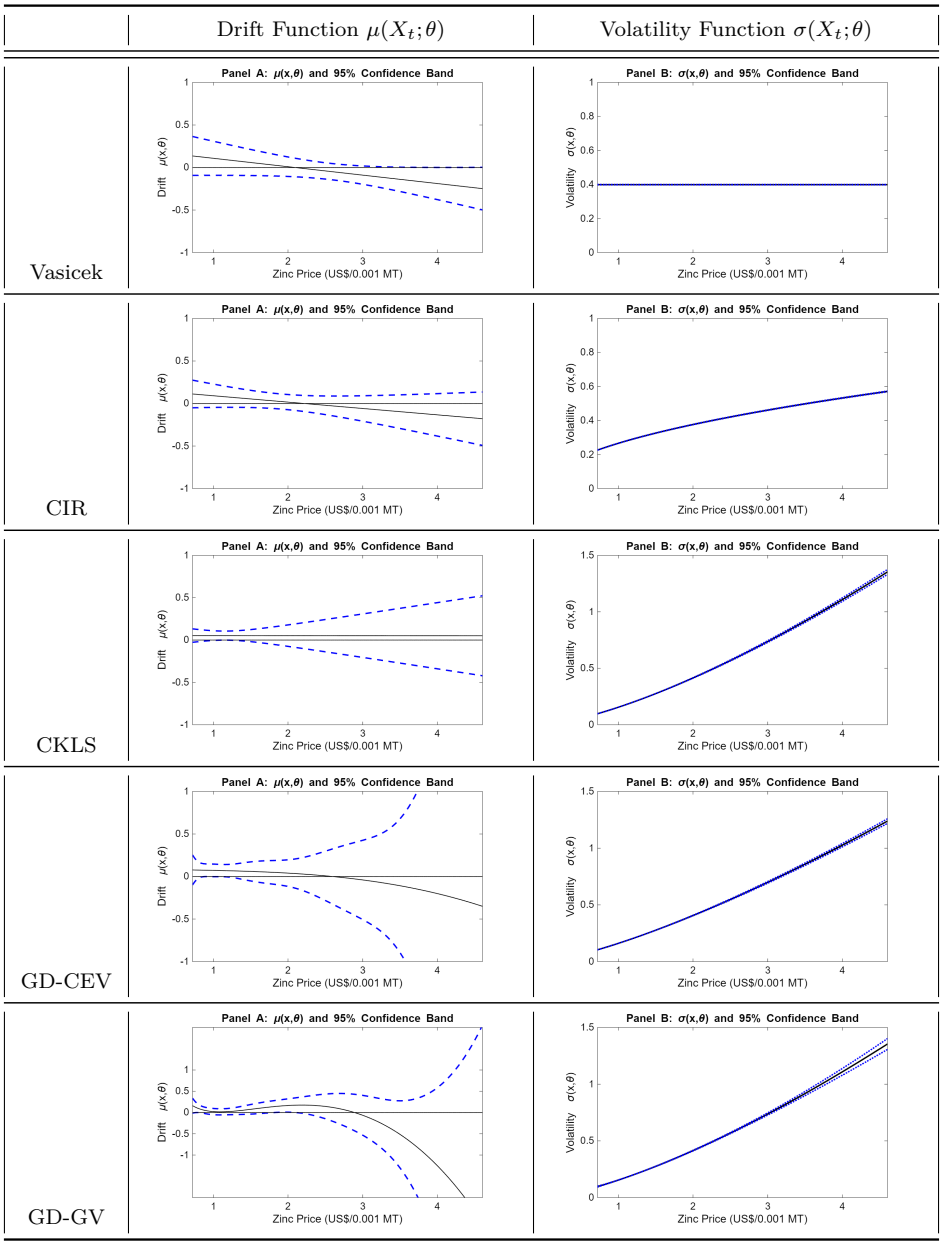

Figure 8: Drift and Volatility Functions for Zinc. The drift and volatility functions were evaluated using the estimated parameters from each diffusion model over the range of observed zinc prices. The dashed lines represent the 95% confidence bands for the estimated functions.

the most suitable. This is because the more complex models (GD-CEV and GD-GV) were not found to be statistically superior, and their drift parameters were largely insignificant. This analysis demonstrates that while all non-ferrous metals share a common dependence on volatility, the specific price dynamics are not homogeneous, necessitating a careful, metal-specific statistical approach.

5. CONCLUSION

This paper empirically investigates the most appropriate continuous-time diffusion models to describe the dynamic behavior of four major non-ferrous metals: copper, aluminum, nickel, and zinc, using daily price data. To this end, five diffusion models—Vasicek, CIR, CKLS, GD-CEV, and GD-GV—were specified, and their parameters were estimated using the maximum likelihood estimation method after deriving approximate transition probability density functions via the method developed by (Aït-Sahalia, 2008).

The estimation results reveal several important similarities and differences in the price dynamics of the four metals. A key commonality is that the price dynamics of all metals are dominated by the volatility function. Volatility-related parameters in all models were found to be highly statistically significant, and volatility consistently showed heteroskedasticity, increasing with the price level. This suggests that the assumption of constant volatility is inappropriate for modeling non-ferrous metal prices.

However, the most appropriate model for each metal differed. For aluminum, the most flexible GD-GV model was selected as the optimal model, based on a comprehensive consideration of the likelihood ratio test and information criteria AIC and BIC. This is supported by the finding that the additional parameters in the GD-GV model's generalized volatility function were statistically significant. Conversely, the price dynamics of copper, nickel, and zinc were best explained by the more parsimonious CKLS model. For these three metals, no evidence was found to suggest that more complex models like GD-GV were statistically superior.

Furthermore, the analysis of the drift function yielded varying results across metals. While a weak tendency towards mean-reversion was observed in aluminum's simpler models, the drift parameters for copper, nickel, and zinc were largely statistically insignificant. This suggests that the role of the volatility function is more critical than that of the drift

function in explaining the price dynamics of non-ferrous metals.

The findings of this study demonstrate that even within the same category of commodities, price movements are not homogeneous, and it is crucial to select a flexible model that fits the specific characteristics of each metal. This provides important implications for risk management in related industries, derivative pricing, and investors' portfolio management.

Future research could explore other models not considered in this paper. For instance, a diffusion model incorporating jump factors could be used to explain sudden price surges or drops, or a multivariate diffusion model could be applied to analyze the interdependence among multiple metals.

REFERENCES

Aït-Sahalia, Y. (1996). "Testing continuous-time models of the spot interest rate," *Review of Financial Studies* 9, 385-426.

Aït-Sahalia, Y. (2002). "Maximum likelihood estimation of discretely sampled diffusions: a closed-form approximation approach," *Econometrica* 70, 223-262.

Aït-Sahalia, Y. (2008). "Closed-form likelihood expansions for multivariate diffusions," *Annals of Statistics* 36, 906-937.

Akaike, H. (1973). "Information theory and an extension of the maximum likelihood principle," in *2nd International Symposium on Information Theory*, Akademiai Kiado, 267-281.

Bates, D.S. (1996). "Jumps and stochastic volatility: Exchange rate processes implicit in Deutsche Mark options," *Review of Financial Studies* 9, 69-107.

Black, F. and M. Scholes (1973). "The pricing of options and corporate liabilities," *Journal of Political Economy* 81, 637-654.

Brennan, M.J. and E.S. Schwartz (1985). "Evaluating natural resource investments," *Journal of Business* 58, 135-157.

Chan, K.C., G.A. Karolyi, F.A. Longstaff, and A.B. Sanders (1992). "An empirical comparison of alternative models of the short-term interest rate," *Journal of Finance* 47, 1209-1227.

Choi, S. (2009). "Regime-switching univariate diffusion models of the short-term interest rate," *Studies in Nonlinear Dynamics & Econometrics* 13, 1-24.

Choi, S. (2013). "Closed-form likelihood expansions for multivariate time-inhomogeneous diffusions," *Journal of Econometrics* 174, 45-65.

Choi, S. (2015a). "Explicit form of approximate transition probability density functions of diffusion processes," *Journal of Econometrics* 187, 57-73.

Choi, S. (2015b). "Maximum likelihood estimation of continuous-time diffusion models for Korean short-term interest rates," *Economic Analysis (Quarterly)* 21, 28-58.

Choi, S. (2020a). "Recent development of closed-form approximate (log-) transition probability density functions of diffusion processes," *Journal of Economic Theory and Econometrics* 31, 97-152.

Choi, S. and J. Lee (2020). "Maximum likelihood estimation of continuous-time diffusion models for exchange rates," *East Asian Economic Review* 24, 61-87.

Cox, J.C., J.E. Ingersoll, and S.A. Ross (1985). "A theory of the term structure of interest rates," *Econometrica* 53, 385-407.

Dias, J.C. and J.P.V. Nunes (2011). "Pricing real options under the constant elasticity of variance diffusion," *Journal of Futures Markets* 31, 230-250.

Dixit, A.K. and R.S. Pindyck (1994). *Investment under Uncertainty*, Princeton University Press.

Dothan, L.U. (1978). "On the term structure of interest rates," *Journal of Financial Economics* 6, 59-69.

Heston, S.L. (1993). "A closed-form solution for options with stochastic volatility with applications to bond and currency options," *Review of Financial Studies* 6, 327-343.

Lo, A.W. (1988). "Maximum likelihood estimation of generalized Itô processes with discretely sampled data," *Econometric Theory* 4, 231-247.

Merton, R.C. (1973). "Theory of rational option pricing," *Bell Journal of Economics and Management Science* 4, 141-183.

Nowman, K.B. and H. Wang (2001). "Modelling commodity prices using continuous time models," *Applied Economics Letters* 8, 341-345.

Paddock, J.L., D.R. Siegel, and J.L. Smith (1988). "Option valuation of claims on real assets: The case of offshore petroleum leases," *Quarterly Journal of Economics* 103, 479-508.

Schwartz, E.S. (1997). "The stochastic behavior of commodity prices: Implications for valuation and hedging," *Journal of Finance* 52, 923-973.

Schwartz, E.S. and J.E. Smith (2000). "Short-term variations and long-term dynamics in commodity prices," *Management Science* 46, 893-911.

Schwarz, G. (1978). "Estimating the dimension of a model," *Annals of Statistics* 6, 461-464.

Yan, X. (2002). "Valuation of commodity derivatives in a new multi-factor model," *Review of Derivatives Research* 5, 251-271.

Vasicek, O. (1977). "An equilibrium characterization of the term structure," *Journal of Financial Economics* 5, 177-188.

Yu, J. (2007). "Closed-form likelihood approximation and estimation of jump-diffusions with an application to the realignment risk of the Chinese Yuan," *Journal of Econometrics* 141, 1245-1280.